Mesoscale Modeling of Deflagration on the Surface of Metalized Solid Fuels

Hong-Suk Choi[1], Jack J. Yoh[1*]

[1]Department of Aerospace Engineering, Seoul National University, Seoul 08826 Korea

Abstract

This study examines mesoscale deflagration, a propagating flame that forms on the surface of a metalized solid propellant. Energy transfer to the adjacent material occurs via convection and diffusion, which are separately handled based on the associated time scale. For convective and diffusive burning, the Arrhenius law is utilized, along with the third order Runge-Kutta method and Essentially Non-Oscillatory (ENO) schemes to discretize the temporal and spatial domain. The interface between two materials is tracked by the level-set function which describes the deforming boundary. The unreacted particles are ignited by the strong compression wave in the convection dominating region while the conduction governs the heat flux in the reaction zone. In particular, the slow flame that includes conductive transfer of heat is handled independently from convective transfer via a large time step scheme. The flame velocity in the simulation is compared to the theoretical value based on the pressure burn rate. Furthermore, the melt layer where the surface burning occurs is reproduced to elucidate the process of surface reaction between the unreacted propellant and exhausting gas

1 Introduction

Aerospace engineers focus on the energy efficiency of fuel because the launch vehicle has been developed to reduce the total weight. Metal has a high energy density compared to conventional solid fuel and is stable to reaction compared to gas and liquid, as such the engineers resort to adding a high amount of metal particles to the baseline solid fuels. However, the complex reaction mechanism on a microscale is hard to understand in detail. Moreover, the metalized solid fuels behave quite differently depending on their particle size. Thus, the investigation on the chemical interaction between metal particles and solids exposed to gas environment has received strong interest in the rocket propellant community.

When the solid fuel is ignited, the entire process from the unreacted solid state to the formation of exhaust gases could be divided into three different regions such as the solid region, the melt layer, and the outflow region. The unreacted metal particles composed of Viton and Graphite are called the 'solid region'. After the solid is fully heated, the metal starts reacting vigorously in the 'melt layer'. A reacted gaseous flame is pushed out from the melt layer to the 'outflow region' owing to the high pressure generation on the burning surface. Sippel et al. demonstrated the three regions for aluminum combustion [1]. Three different kinds of flames are generated when the solid propellant undergoes combustion with metal components: primary premixed flame, primary diffusion flame, and final diffusion flame [2]. This paper enunciates the flame structure and highlights the combustion mechanism on the solid propellant in the mesoscale [2].

Similar studies have focused on the outflow region where the complex turbulent gas could be observed [2,3]. It is paramount to understand the metal particle reaction process and temperature dependency in the melt layer. Kim et al. modeled the after-burning of Al particles triggered by highly compressible pressure from energetic material on the micro scale [4]. Even though it didn't specifically address the melt layer, this research is still meaningful because of its scale. Showing the mesoscale combustion of metal particles could be the motivation to pursue this paper.

This study aims to model mesoscale combustion on the melt layer and study the chemical and mechanical behavior of solid fuel, which is heterogeneously metalized. Here, a numerical domain was employed to simulate the combustion of micro metal particles. Zirconium Potassium Perchlorate (ZPP) (52wt% Zr, 42wt% KClO4, 5wt% Viton B, 1wt% graphite) is used as a solid fuel, Zirconium (Zr) with potassium perchlorate (KClO4) is used as a metal particle, and the binder is a mixture of Viton B and graphite. The variation of temperature during convective and diffusive burning are presented with a different time scale in surface burning.

2 Methodology

2.1 Governing equation

The mesoscale deflagration of propagating flame on the surface of metalized solid is modeled using 2-D Euler equation along with Arrhenius law. The governing equation and each matrix components of the Euler equation are defined below

$$\frac{\partial U}{\partial t} + \frac{\partial E}{\partial x} + \frac{\partial F}{\partial y} = S(U) \tag{1}$$

$$U = \begin{bmatrix} \rho \\ \rho u_x \\ \rho u_y \\ \rho E \\ \rho \lambda \end{bmatrix}, \quad E = \begin{bmatrix} \rho u_x \\ \rho u_x^2 + P \\ \rho u_x u_y \\ u_x(\rho E + P) \\ \rho \lambda u_x \end{bmatrix}, \quad F = \begin{bmatrix} \rho u_y \\ \rho u_x u_y \\ \rho u_y^2 + P \\ u_y(\rho E + P) \\ \rho \lambda u_y \end{bmatrix}$$

$$S = \begin{bmatrix} 0 \\ 0 \\ 0 \\ \rho Q \dot{\lambda} \\ \rho \dot{\lambda} \end{bmatrix} \tag{2}$$

Here, U is the matrix of conservative variables, E and F are the

matrices of flux along X and Y-direction respectively, and S is the matrix of the source term. The conservative variables ρ, u_x, u_y, E, and λ signify the density, x-direction velocity, y-direction velocity, total energy, and reaction rate of ZPP respectively, P designates the pressure here, and the heat of reaction is expressed as Q.

2.2 Numerical technique

The time is discretized by the third-order Runge-Kutta method, and two-dimensional space is discretized by the ENO scheme [3].

Equation of State (EOS) is used to compute the pressure of unreacted metal particles and reacted hot gas. Nobel-Abel EOS is used for the exhaust gas, while Tait EOS is utilized for metal particles. Each equation is written out as follows [5].

$$P_u = B\left(\left(\frac{\rho}{\rho_0}\right)^N - 1\right) + A \qquad (3)$$

$$P_r = \frac{(\gamma-1)e}{v-b} \qquad (4)$$

Equation (3) is Tait EOS for liquid and eqn. (4) is Nobel-Abel EOS for gas. Where, B, A, and N in (3) are the Tait EOS coefficients, while b in (4) is the co-volume of fluid. During the chemical reaction, the unreacted particles and exhaust gas are mixed. So pressure at one grid is defined as the mass fraction combination of each calculated pressure.

The speed of sound based on pressure is defined as follows.

$$c^2 = \frac{\partial P}{\partial \rho} \qquad (5)$$

Each material's sound speed is calculated based on its EOSs. The same as pressure, the sound speed is determined by the mass fraction. In this shock-capturing scheme, the global time step is dependent on the eigenvalues that contain the speed of sound. The time step is defined below

$$\Delta t < CFL \frac{\Delta x}{\max(u+c,u,u-c)} \qquad (6)$$

The time step is affected by Courant-Friedrichs-Lewy(CFL) condition. Because the uniform grid length is 10^{-6} m, the CFL number is maintained under 0.6. The maximum absolute value of the velocity component is obtained from eqn. (6).

The chemical reaction models employ the single-step Arrhenius rate law

$$\frac{\partial \lambda}{\partial t} = A\exp\left(-\frac{E_a}{RT}\right) \qquad (7)$$

Where Ea is the activation energy, A is the pre-exponential component and R is the universal gas constant. Using an in-house calorimeter, the value of A is found to be exp(30.4)s-1, and the value of Ea is 213 kJ/mol [6]. This simulation is performed using in-house code (C#) which has a unique algorithm developed in the laboratory.

2.3 Numerical domain, initial and boundary conditions

The numerical domain has dimensions of 0.3 mm × 0.6 mm in the x and y directions and is discretized into 180,000 cells (300 × 600) using a uniform mesh with a grid size of 1μm × 1μm. The lower boundary has an end wall condition, whereas the others have zero gradient boundaries. The comprehensive domain shape is shown in Fig. 1.

In the modeling of ZPP, Graphite and Viton serve as the binder,

whereas the mixture of KClO$_4$ and Zr represents the particle. These particles are spherical in shape and have an average diameter of 48 mm. Approximately, 80 particles are randomly distributed in the numerical domain. The upper boundary's 20% region is heated to 1300 K from a starting temperature of 300 K because the reaction of ZPP starts near 1400 K in the 0-D simulation.
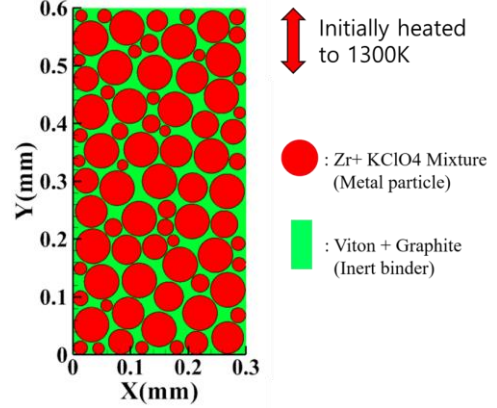

Figure 1: Mesoscale simulation contour of ZPP

2.4 Interface tracking method

It is necessary that if more than two materials interact with each other, the interface between the materials must be clearly defined. The distance between the node and the nearest boundary is defined with a level-set function, φ, which is calculated by Euler's conservation equation as follows [7].

$$\frac{\partial \varphi}{\partial t} + \frac{\partial(\varphi u_x)}{\partial x} + \frac{\partial(\varphi u_y)}{\partial y} = 0 \qquad (8)$$

The sign of the level-set function is defined based on the type of interface between two materials. First, all boundaries of materials are expressed as zero level-set. Figure 2 shows the schematic of the level set function identifying the boundaries of two materials. Here, it is considered that for $\varphi < 0$, the node is inside the material, whereas for $\varphi > 0$, the node is outside the material. So the level-set function is dependent on the material and the distance from the boundary. And each material has its level-set function. This implies that when the level-set function is defined in the code, the Euler conservation equation should be conducted for both of them.
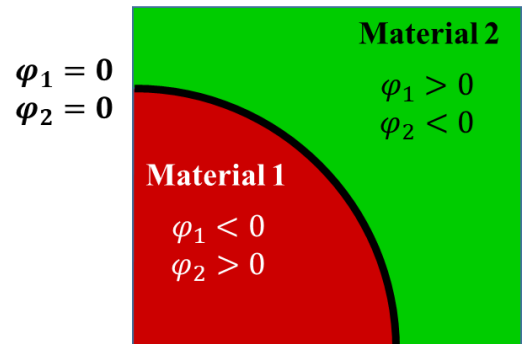

Figure 2: Schematic demonstration of the level-set function definition

3 Results

3.1 Simulation result

Since the particles were randomly generated in the domain, the maximum pressure point is variable for initial distribution. However, the maximum pressure was maintained at 150 MPa, while the burning surface pressure was maintained at 50 MPa. Figure 3 shows the temperature contour showing the convective burning. It is observed that, after the particles were heated to 1300 K, the temperature inside of the material increased slowly to 1400 K. And the temperature dramatically increased to the maximum when the temperature reached 1400K. By this increasing pattern, the fast combustion showed the high-speed deflagration pressure in Fig. 3.
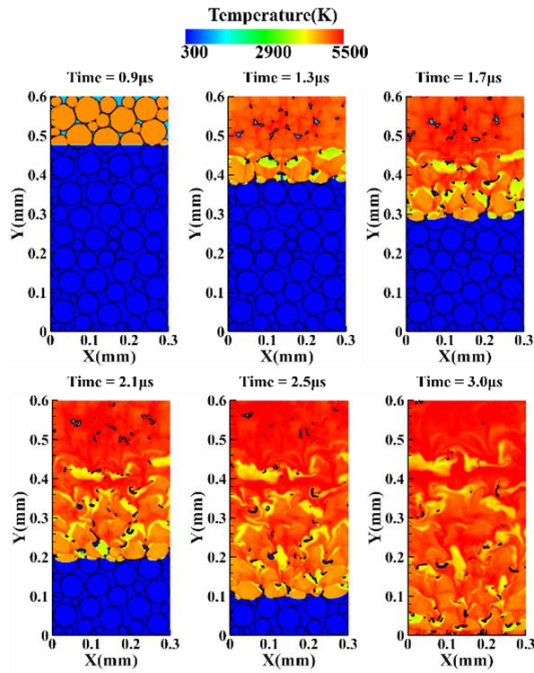

Figure 3: The variation of temperature during the convective burning
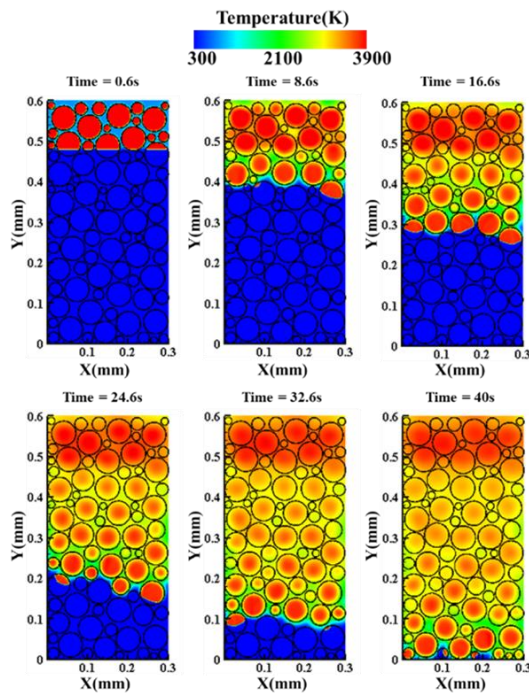

Figure 4: The variation of temperature during the diffusive burning

Convection dominates fast combustion and diffusion dominates slow combustion, here both phenomena are considered. Fig. 4 shows the variation of temperature during the diffusive burning. During convective burning, the maximum temperature of the hot gas product reaches up to 5500K as compared to slow combustion (Fig. 4.) where the maximum temperature is limited to 3900 K. The maximum temperature is higher for fast combustion because of the complexity of the hydraulic interaction of the products and reactants. Moreover, the heat of reaction flows out of the reacted particles by diffusion as observed in Fig. 4. This process is achieved in 40s while the fast deflagration completely burns the entire particles within 3μs. When the particle reaction is simulated in 0-D condition using the same activation energy and pre-exponential factor, the reaction temperature is approximately 4700 K. This temperature is the median value of two results, and if the pressure interaction and conduction are considered, the temperature results seem to be valid.
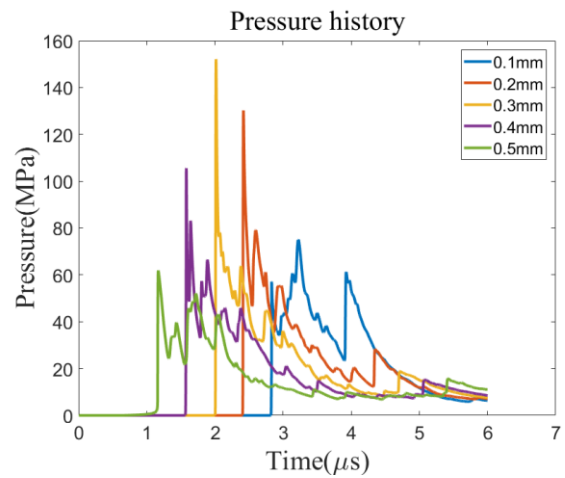

Figure 5: Pressure history of the midpoint in the x-direction at 0.1, 0.2, 0.3, 0.4, and 0.5 mm above from bottom

The pressure history in convective burning is shown in Fig. 5. Each graph of different color represents the pressure of the midpoint in the x-direction in a 0.1 mm gap from the bottom. Because of the randomness of the particles, the maximum pressure of each point doesn't have a tendency to distance from the top. The more particles are concentrated near the point, the higher maximum pressure is formed by shock wave overlapping.

3.2 Time scale validation

Equation (6) shows that the time step is dependent on the grid length, the speed of sound, and the velocity. So in convective burning, the time step is in the nanosecond scale range. On the other hand, the convection was ignored in diffusive burning: the time step in this simulation was not affected by the CFL condition. The calculated time scale of each simulation is presented in Table 1.

It is observed that when the pressure range is between 10 to 100 MPa, the burning rate of ZPP is about 50-170 mm/s [3]. So, the 0.6 mm of ZPP propellant should be reacted completely in 3~10 ms. The theoretical burn rate is the approximate median value of two conducted simulations. Therefore, to validate the combustion simulation, activation energy, and pre-exponential factor should be adjusted to experimental value when the time step problem is solved.

Table 1: Time scale of mesoscale surface burning simulations

Condition	Time scale (s)
Fast deflagration simulation	$10^{-9} \sim 10^{-8}$
Diffusion dominating simulation	$10^{-2} \sim 10^{-1}$
Slow deflagration simulation	$10^{-6} \sim 10^{-5}$

4 Conclusions

Metalized solid fuel (ZPP) was subjected to mesoscale surface combustion modeling in this study. A theoretical rate law was used to evaluate the reactivity of metalized propellant in the melt layer, and the generation of exhaust products including solid by-products and gas is investigated. The chemical and mechanical interactions between the reacting particles and the exhaust gas on the burning surface are illustrated analytically. This study presents a novel approach by demonstrating the deflagration that occurs on the melt layer generated by a chemical reaction in particles comprised of both metal and oxidizer at the mesoscale However, to validate the simulation result with the theoretical burn rate, reducing the approximation and using the experimental values for the chemical reaction are required. Moreover, because the time scale of the theoretical value is much smaller than the simulation scale, the CFL condition and stiffness problem must be overcome. A fully implicit convection scheme and physics-informed deep learning based on time have been suggested in future study. The multi-time step integrator that treats both slow and fast flame will be developed and presented during the conference.

References

[1] T.R. Sippel, S.F. Son, L.J. Groven, S. Zhang, and E.L. Dreizin, Combustion and Flame, 162 (2015), 846-854.

[2] M.W. Beckstead, R.L. Derr, and C.F. Price, AIAA J, 8 (1970), 2200-2207

[3] S.H. Choi, B.H. Kim, S.Y. Han, and J.J. Yoh Combustion and Flame., 221 (2020), 401-415

[4] B.H. Kim, S.H. Choi, and J. J. Yoh, Combustion and Flame., 210 (2019), 54-70

[5] A. Chiapolino and R. Saurel, Fluids., 3 (2018), 48

[6] H.L. Friedman, Journal of Polymer Science, 6 (1963) 183-195

[7] K.H.Kim and J.J. Yoh, Journal of Mathematical Physics., 49 (2008), 043511